Combustion and Flame 231 (2021) 111469

Contents lists available at ScienceDirect

Combustion and Flame

journal homepage: www.elsevier.com/locate/combustflame

Experimental study on sooting propensities of ternary blends of n-dodecane, isododecane, and C8 oxygenates at high pressures

Irene Ruiz-Rodriguez [a,*], Roger Cracknell [b], Michael Parkes [b], Thanos Megaritis [a], Lionel Ganippa [a]

[a] Brunel University London, Mechanical, Aerospace and Civil Engineering Department, UB8 3PH, United Kingdom
[b] Shell Global Solutions, Shell Centre, 4 York Road, Lambeth, SE1 7NA, United Kingdom

ARTICLE INFO

Article history:
Received 5 November 2020
Revised 8 April 2021
Accepted 9 April 2021
Available online 15 May 2021

Keywords:
Oxygenated fuels
Soot
Spray combustion
Constant volume chamber
Soot natural luminosity

ABSTRACT

The use of liquid fuels in internal combustion engines is still prevalent in society because of their high energy density, ease of handling, and matured engine technology. Along with other power generation sectors, the transport sector faces the need to reduce emissions such as soot. One option to address this is to use oxygen-bearing fuels. The presence of oxygenated compounds in fuels have the potential to reduce soot emissions in heavy duty diesel engines and various power generation sectors. Understanding the fundamental combustion and sooting characteristics of oxygenated compounds at high pressures is essential for the development of future low sooting fuels. In this work, four oxygenated compounds belonging to the C8 functional group were deployed along with normal dodecane and isododecane to form ternary blends having the same oxygen content, of 2.5% by mass, and a matching cetane number of 52. The blends were injected at a high pressure into controlled high pressure, high temperature conditions in a constant volume chamber. The flame and the soot natural luminosity were investigated with high-speed diagnostics. The results revealed that the blends delayed the onset of the first appearance of soot. The presence of oxygenates increased the soot lift-off length by 40%, hindered the formation of soot by up to 55%, and enhanced the oxidation by up to 10%, all relative to diesel. The sooting tendency of the oxygenated blends increased in the order of ketone ≈ alcohol < ester < aldehyde < diesel. The difference between the sooting tendencies of the oxygenates was smaller than those between the oxygenates and diesel, showing that soot reduction was mostly due to oxygen content and dilution effects. However, the small differences observed between the oxygenates indicates that the moiety does have an effect on soot reduction—but to a lesser extent than dilution and oxygen effects.

1. Introduction

Liquid fuels have high energy densities and they are relatively easy to store and handle; hence they suit the current fleet of engines, which have been optimised for their use [1]. Internal combustion engines (ICEs) that utilise liquid fuels are prevalent in society, and they are well suited for demanding applications such as heavy duty, off-road, maritime, aviation, and military. Despite their high thermal efficiency and power output, the in-cylinder production of emissions from the combustion process of traditional hydrocarbon fuels is under scrutiny, and ways are continuously sought to reduce the in-cylinder formation of pollutants [1]. One emission of concern is soot, which not only reduces the combustion efficiency but also affects the environment [2,3]. Engine-out soot emissions affect adversely the environment, but in modern engines this can be taken care of by the use of aftertreatment systems. However, addition of aftertreatment systems to reduce NOx and soot emissions can incur fuel penalties and carbon emissions; hence there is a greater need to understand and minimise soot formation from in-cylinder processes. A promising strategy for the reduction of emissions in current engine infrastructures is to design future fuels with appropriate C/H/O content having optimal thermal, physical, and chemical properties [4–8].

The presence of oxygen in hydrocarbon fuels has the potential to alter the reaction pathways leading to the formation of soot and those enhancing its oxidation [4–8]. To facilitate the implementation of oxygenated fuels in current engine technology, oxygenates must be evaluated and blended with a base fuel at an optimum concentration. Several works have focused on studying the soot-

* Corresponding author.
E-mail address: irene.ruizrodriguez@brunel.ac.uk (I. Ruiz-Rodriguez).

https://doi.org/10.1016/j.combustflame.2021.111469

ing properties of blends containing short carbon-chain oxygenated compounds such as ethanol, butanol, dimethyl ether (DME), acetone, and pentanone amongst others [5,9–11]. However, the thermal, physical, and chemical properties of short carbon-chain oxygenates are very different from those of diesel. Limited works have been performed under engine-like conditions to explore the combustion of long carbon-chain oxygenates, which tend to have similar properties to those of diesel and show potential to reduce soot [12].

The combustion of neat di-n–butyl–ether (DNBE) and octanol was studied in a single-cylinder engine in [6], where it was shown that DNBE has a shorter ignition delay than octanol. Even though both oxygenates have the same amount of oxygen content, their chemical structure is different, and this affected the combustion process, which led DNBE to produce lower hydrocarbon emissions. Other emissions such as CO and NO_x were also studied in their work. For CO emissions, an inverse correlation with the fuel cetane number (CN) was proposed, whereas for NO_x, no significant differences were reported. Numerical investigations have been performed in [5] to study the effect of oxygenated compounds such as tri-propylene glycol methyl ether, dimethyl ether, and methyl decanoate on combustion and soot emissions in high pressure sprays from a single hole nozzle under engine operating conditions. It was shown that the fuel molecular structure can alter soot formation, and that with an increase in oxygen content the formation of soot precursors can be reduced. In [12] and [13], the soot and combustion characteristics of four different oxygenates with a C8 carbon-chain were studied under high ambient temperatures. It was shown that all oxygenates reduced soot emissions relative to diesel whilst maintaining a similar flame temperature. It was also shown that soot reduction was partly controlled by dilution effects, caused by the absence of aromatics and long carbon-chain aliphatics. Oxygen content and, to a lesser extent, the chemical effect of different oxygenate moieties, also played a role in soot reduction. Thus, these effects must also be considered when looking at the mechanisms behind soot reduction of oxygenates.

Whilst studies on the combustion of neat oxygenates are needed to build a database on their properties and to understand the fundamental mechanisms underlying soot reduction, to reap the benefits of soot reduction with the current engine technology on a short- to mid-term basis, a gradual introduction of oxygenates as part of a blend is required. Studying the combustion properties of oxygenates in a blend is thus essential to determine the extent of their soot reduction capabilities and the mechanisms through which this is achieved. Few studies have been performed to explore the combustion properties of long carbon-chain oxygenate blends in open flames, shock tubes, constant volume chambers, or in engines [14–18]. Some make use of the Oxygen Extended Sooting Index (OESI) to quantify the sooting tendency when testing using smoke point measurements, which accounts for the oxygen content in the oxygenated fuels studied, as presented and detailed in [18]. For example, the sooting propensity of C4 and C5 oxygenates have been studied in turbulent diffusion flames by blending them with a diesel surrogate [14]. Based on their measured sooting index, it was shown in [14] that oxygen moieties have an effect on sooting propensity, with an increase in the order of esters < aldehydes < ketones < alcohols. It was also shown that the position of oxygen in the fuel structure influenced the production of soot, and that moving the moiety towards the centre of the fuel structure limited the formation of soot.

In [15], a combination of in-cylinder imaging and exhaust soot measurements were used to determine the sooting propensity of blends of synthetic diesel with dibutyl maleate, cyclohexanone, and anisole, all having a 9% oxygen content. Their optical engine studies revealed that both pre-mixing and chemical composition influenced the formation of soot, and that a longer pre-mixing time normally favours a reduction in soot. Studies in engines with diesel-oxygenate blends using oxygenates such as C8 and C10 alcohols, rapeseed methyl ester (RME), ethanol, diglyme, dimethoxymethane, and several esters also show potential in terms of soot reduction without a significant compromise in engine performance [16,17].

The soot reduction potential of oxygenates has been demonstrated in numerous works, either as neat fuels or as part of a blend; not many of them have focused on systematic matching of the cetane number of fuel blends containing different oxygen moieties whilst maintaining the same percentage of oxygen content. This kind of systematic investigation is presented in this work, and it allowed to determine to what extent the effect of pre-mixing, oxygen content, and chemical moiety affect the sooting propensity of the oxygenates. Furthermore, experimental works that provide spatio-temporal information on the development of soot in high pressure spray flames are limited for these types of fuel blend compositions (long carbon-chain oxygenate blends with matching cetane number and oxygen content), and they are needed to understand the fundamentals of the processes of potential drop-in fuels. These experimental data could also be useful for developing chemical kinetic models concerned with soot processes for complex fuel blends.

This work investigates the combustion and sooting characteristics of four long carbon-chain oxygenated compounds, namely, 1-octanol, 2-octanone, hexyl acetate, and octanal, as part of ternary blends with two base compounds: isododecane (2,2,4,6,6-pentamethylheptane) and n-dodecane. These oxygenates were selected because of their potential to reduce soot as neat components [6,12,13,19,20], because of their similar thermo-physical properties to diesel, and because of their potential to be manufactured sustainably [21–23]. All blends were designed to have the same cetane number (CN) and oxygen content and were studied under ambient temperatures and pressures typical of engine-like conditions. Natural soot luminosity (NL) was acquired at a high-speed to understand the combustion behaviour of these blends and to elucidate the extent of soot reduction of different moieties in a ternary blend. In addition to soot, one could also wonder what impact fuelling with oxygenates might have on other emissions, for example on NO_x. Whilst some studies have shown that under specific engine conditions it is possible to keep NO_x levels within regulation limits when using oxygenates [6], because of its dependence on other properties such as flame temperature and exhaust gas recirculation (EGR), other emissions must be tested for specifically. In this work, we focus on the combustion characteristics and development of soot. Other emissions are not within the scope of this study but could certainly be an interesting area of work for future research.

The paper is organised as follows: in Section 2, the fuels, set-up, and procedures used are described; in Section 3, the results and discussions are presented, divided into four subsections: the first one discusses the combustion characteristics of the blends, the second one the interpretation of the natural luminosity, the third one quantitatively analyses the sooting trends for the full combustion event, and finally the fourth one looks at mechanisms that are responsible for the observed trends; in Section 4, the conclusions and findings of this work are summarised.

2. Experiments and diagnostics

2.1. Fuels

Four different oxygenated compounds were tested in ternary blends to understand how soot propensity changes with different moieties. The oxygenated compounds studied, 1-octanol ($C_8H_{18}O$), 2-octanone ($C_8H_{16}O$), hexyl acetate ($C_8H_{16}O_2$), and oc-

Table 1
Blending ratios by volume of the oxygenates, isododecane, and n-dodecane. Blends all have a matching derived cetane number of 52 and a fixed oxygen content of 2.5% by mass.

Oxygenate	Oxygenate concentration (v/v%)	N-dodecane concentration (v/v%)	Isododecane concentration (v/v%)	Blend abbreviation
1-octanol	19	46	35	BOL
2-octanone	19	42	39	BONE
hexyl acetate	10	47	43	BHA
octanal	19	30	51	BAL

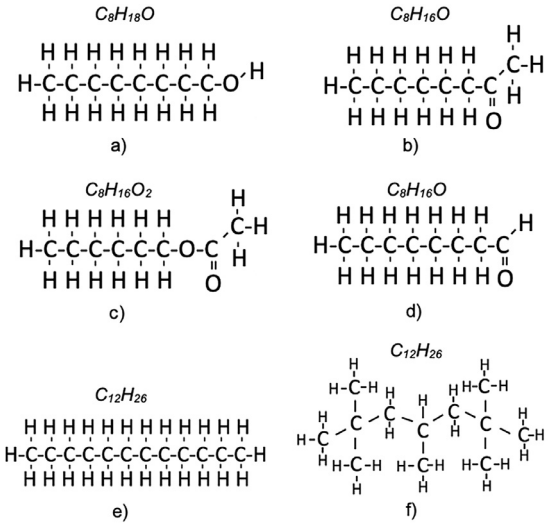

Fig. 1. Chemical structure of the components used as part of the ternary blends. a) 1-octanol, b) 2-octanone, c) hexyl acetate, d) octanal, e) n-dodecane, f) isododecane.

Table 2
Measured and calculated physical properties for the blends studied in this work. For the values measured, the density was obtained at 15 °C and the viscosity at 40 °C. [a]Calculated as an approximation, [b][24],[c]Measured,[d]EN590 specifications.

Fuel	Lower Calorific Value (MJ/kg)	Density (kg/m^3)	Viscosity (cST)
BOL	44[a]	766[c]	1.7[c]
BONE	44[a]	764[c]	1.2[c]
BHA	44[a]	763[c]	1.3[c]
BAL	44[a]	765[c]	1.3[c]
Diesel	43[b]	820–845[d]	2–4.5[d]

tanal ($C_8H_{16}O$), have a carbon backbone chain of eight but different molecular structures, as shown in Fig. 1.

All the oxygenates were blended with isododecane (2,2,4,6,6-pentamethylheptane) and n-dodecane to obtain a derived cetane number (DCN) of 52 and a mass oxygen content of 2.5%. This DCN closely resembles that of EN590 diesel (as used in this work) based on the ASTM D7668. The blending ratios by volume can be seen in Table 1, and the oxygenated blends have been named: BOL (1-octanol blend), BONE (2-octanone blend), BAL (octanal blend), and BHA (hexyl acetate blend). The uncertainty in the mixture composition due to blending remained within 10% of the reported values. The blending ratios were obtained by testing different mixture compositions following the standard IQT, for which details can be found in the standard ASTM D6890. Diesel was used as reference fuel for a relative comparison with the oxygenated blends. Table 2 shows the physical properties obtained for the blends. The lower calorific values (LCVs) were computed on an additive basis, the densities were measured using the standard ISO 12185 method, and the viscosities were measured using the standard ISO 3104 method. For diesel, the values of these properties were obtained from the stated references in literature.

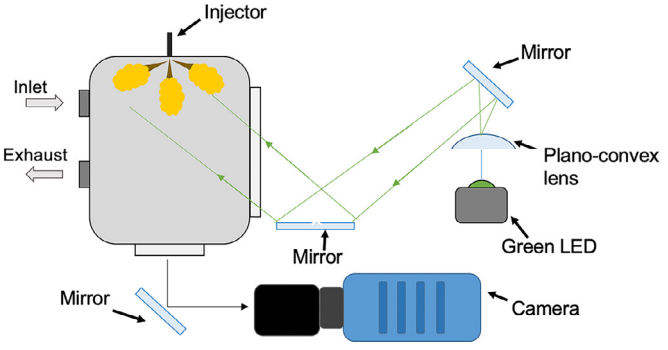

Fig. 2. Set-up used to collect the data. Fuels were injected into the controlled ambient conditions of the constant volume chamber and the data were recorded using high-speed imaging. Note that in the actual set-up all six holes in the injector point out radially.

2.2. Experimental set-up and diagnostics

A diagram of the set-up used in this work is presented in Fig. 2. The sooting propensity of the ternary blends and diesel were evaluated by injecting the fuels at 700 bar into a constant volume chamber (CVC) using a solenoid-actuated, six hole, multi-hole injector. The CVC was pressurised and heated to engine-like conditions through chemical preheating. This was achieved by filling the chamber with C_2H_2 and igniting the mixture with a spark plug. After ignition, both temperature and pressure rise, and thereafter experience a decay. The fuel injection was triggered at the desired temperature and pressure during this decay. This procedure was automated, and it was controlled and monitored by a synchronisation system. The ambient oxygen concentration, pressure, and temperature in the CVC at the time of injection were 10%, 25 bar, and 940 K, respectively. This relatively low ambient oxygen concentration resembles high EGR conditions in an engine. The repeatability of the ambient conditions in the chamber after chemical preheating was of 98%. The fuel injection duration was maintained at 1.5 ms and the energy content of the fuels were comparable. This similarity in LCVs between the blends tested and diesel could be beneficial in terms of fuel efficiency. From Table 2, it can be seen that diesel's density is slightly larger than for the blends, which could raise questions about differences in fuel injected. It is noted from simple physical correlations that, provided the nozzle size and pressure drop remain unchanged (as in this work), the theoretical mass flow rate is proportional to the square root of the density. Thus, the overall mass difference between diesel and the blends will be within 3%, which is not expected to have a significant impact on the sooting trends.

The CVC has two optical accesses, one by the side and one at the bottom. The side window allowed for illumination of the sprays using a high-power green LED, which was useful to separate the sprays from the flame during post-processing. Below the bottom window, a mirror was placed to image the combustion event onto the high-speed CMOS camera. The camera was operated at 19,200 frames per second (fps), with an imaging area of 896 × 792 pixels^2, and a resolution of 109 µm per pixel. The ex-

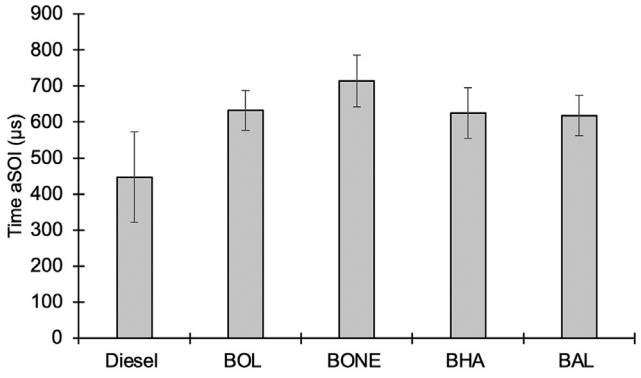

Fig. 3. Average start of combustion (SOC) considered as the first time that soot appears aSOI. Soot normally appears as random pockets that quench rapidly. Injection duration for all fuels was 1.5 ms. Error bars cover two standard deviations from the mean.

posure time was set at 7.5 µs. These settings enabled capturing of the natural luminosity signal of the low sooting fuels whilst avoiding saturation of the camera when combusting high sooting fuels. Saturation of the camera occurs when the pixel charge has reached its maximum value, for example when a flame region is very sooty and produces high intensity values. Though camera saturation was avoided by optimising the set-up, some high intensity regions were still observed for a small percentage of the flame. It was important to quantify these saturation regions to characterise the related uncertainties, as these are regions that are potentially producing more soot than that captured by the detection system. In this work, on average, the maximum percentage of the flame that showed saturated values did not exceed ~ 2% for diesel and ~ 0.3% for the oxygenates.

3. Results and discussion

The results and discussion section has been divided into four parts. In the first part, Section 3.1, combustion characteristics such as the start of combustion (SOC) based on the first appearance of soot luminosity; the soot lift-off length (sLOL); and the end of combustion (EOC) based on the last appearance of a soot cloud, have been characterised for the different fuels. In the second part, Section 3.2, the interpretation of the signal obtained from soot natural luminosity is discussed. In the third part, Section 3.3, the spatio-temporal development of soot from inception to oxidation is discussed for the different blends. Finally, in Section 3.4, hypotheses on possible chemical pathways that might have resulted in the different trends observed in Section 3.3 are investigated.

3.1. Combustion characteristics

The first appearance of soot averaged over all the injections performed for diesel and the blends studied is shown in Fig. 3. In this work, the start of combustion (SOC) was considered to be the time instant at which the local soot luminosity was first visualised as pockets of soot, as shown in Fig. 4. These pockets of soot formed before soot had time to stabilise, when the local conditions in the chamber were reactive enough to promote the formation of soot. The local mixing regions at the periphery of the spray are sensitive to ambient conditions, and the reactivity of the mixture is influenced by the chemical composition and the local temperature. These pockets were observed to be transient and appeared relatively close to the injector, where the head vortex and recirculation zones are prevalent during the early injection stages. In some instances, these local soot pockets quenched as the spray combustion developed. It is noted that the SOC used in this work reflects how long it takes for any point in the mixture to be sufficiently reactive to form soot. This mostly occurred simultaneously in more than one spray, and the occurrence of soot in any of the remaining non-sooting sprays followed shortly after. For diesel, these local pockets were found to be closer to the nozzle than for the other fuels, and also appeared relatively earlier, at ~ 450 µs aSOI. This was followed by BAL, BHA, BOL, and BONE, taking ~ 620 µs, ~ 625 µs, ~ 630 µs, and ~ 715 µs, respectively. All oxygenated blends showed a delayed SOC relative to diesel, which indicates that soot-forming conditions and reactions were slightly retarded for the blends for the considered ambient condition. The differences in oxygenate moieties did not seem to have a major effect on fuel cracking, hence the difference in SOC remained within a standard deviation of one another.

The soot lift-off length (sLOL) is the distance from the nozzle tip to the most upstream location of soot in the spray flames, where soot reactions have stabilised. The sLOL was averaged for all the six sprays over the stable period for the seven injection events performed for diesel and for each blend, as shown in Fig. 5. Relative to diesel, all blends increased the sLOL by approximately 40%, indicating that the oxygenates present in the blend delayed the onset of soot formation and pushed soot to a more downstream location. Dilution effects (i.e., replacement of highly sooting components such as aromatics, by lower sooting components such as linear or branched alkanes) and oxygen effects seemed to play a more important role on soot stabilisation than pre-mixing effects. This is because even though all fuels had a similar CN, including diesel, all oxygenated blends showed a longer sLOL. This also indicates that the oxygenated blends tend to soot less than diesel from the very early reaction stages. A longer sLOL can also have an important implication on oxidation processes, as soot will have less time to accumulate and grow, meaning that there can potentially be less amount to oxidise. Fast oxidation reactions are important to improve soot burn-out, to enhance combustion efficiency, and to reduce engine-out soot emissions.

Relative to diesel, dilution effects had an important influence in delaying the sLOL for the blends. When comparing the sLOL between the different oxygenated blends, the effect of oxygen content on soot stabilisation seemed to be greater than the effect of different functional groups. As shown in Fig. 5, for the same oxygen content, the differences in sLOL were larger between diesel and the blends than between the blends themselves, which showed no statistically significant differences. It is also interesting to note that the standard deviation of the average sLOL value was slightly larger for all oxygenates than for diesel, with variations between 6% and 10% for the former, and 4% for the latter. The presence of oxygen in the fuels not only delayed the onset of soot-forming reactions, but also increased the spatial range where soot could stabilise.

The presence of fuel-bound oxygen influences the rate of combustion, and this can be explored by characterising the end of combustion using the high-speed camera data. The end of combustion (EOC) is a useful parameter that indicates the oxidation propensity of each fuel, and it also provides quantitative information on timescales for complete oxidation, Fig. 6. The EOC was determined from the high-speed data, and is defined in this work as the point in time when the soot from the main combustion event has fully oxidised (excluding soot from EOI expulsions). For the similar injection timings studied, the average values of the EOC for the oxygenates did not vary significantly and remained mostly within a SD. However, on average, the soot produced from combustion of the oxygenated blends oxidised ~ 10% faster than for diesel. This shows that the oxygen content and dilution effects have a stronger influence than the effect of the moiety itself, not only on the formation of soot but also on its oxidation. With respect to diesel, the slightly faster soot oxidation observed for the oxygenates could be associated with the initially reduced amount of soot that was

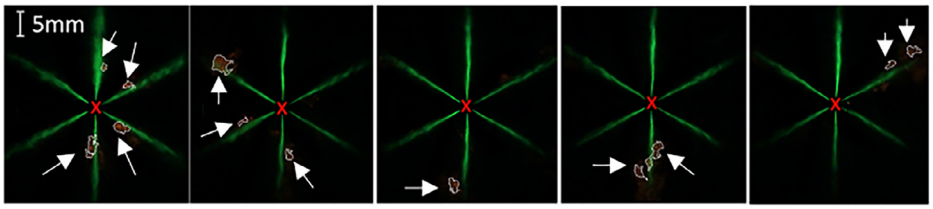

Fig. 4. First appearance of soot pockets for the different fuels studied. Image brightness and contrast have been enhanced for ease of visualisation. The arrows mark the first appearance of soot pockets and the red cross the location of the nozzle. From left to right: diesel at 468 µs aSOI, BOL at 624 µs aSOI, BONE at 728 µs aSOI, BHA at 676 µs aSOI, and BAL at 676 µs aSOI.

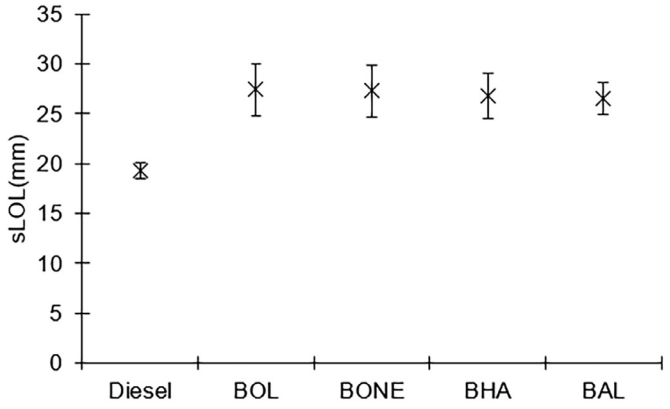

Fig. 5. Soot lift-off length averaged over the six sprays imaged. The error bars represent two standard deviations from the mean.

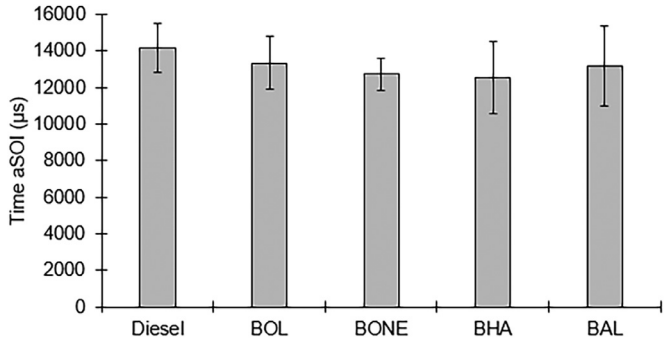

Fig. 6. Average end of combustion (EOC), when the last soot cloud was observed. Error bars cover two standard deviations from the mean.

formed, along with a faster oxidative reactivity of the formed soot. The earlier EOC and shorter combustion duration for the blends can be advantageous in engine applications, as soot can potentially oxidise before the charge exits the engine. From the SOC and EOC results, the oxygenates showed a stronger effect on delaying the SOC than on advancing the EOC, which implies they had a larger effect on delaying the formation of the initial soot pockets during early combustion stages than on enhancing the oxidation of the final soot pockets during the end of combustion.

3.2. Natural soot luminosity and flame temperature

The acquired spray flame images are a 2D representation of a 3D flame, so each pixel represents the accumulation of the intensity from all the sooting particles along the line-of-sight. For highly sooting fuels, such as diesel, use of the natural luminosity of the flame might result in an under-estimation of the total soot because of soot attenuation across the flame. Whilst this is a limitation of any line-of-sight method, it is not expected to have a significant impact on the interpretation of the results presented below, except in that soot reduction values for the oxygenates have to be taken to be conservative. Furthermore, to minimise any impacts of this on the discussion, results are also presented relative to diesel. The natural soot luminosity has to be interpreted with care, as an increase in signal intensity can be either due to an increase in temperature or due to an increase in the local soot concentration at a certain temperature. The spatially integrated natural luminosity (SINL) is dependant on the flame's adiabatic temperature, and flames that produce the same volume fraction of soot but have different flame temperatures can result in different emission intensities [25,26]. Thus, while soot radiative loses are neglected in the computation of the adiabatic flame temperature, the results in Fig. 7 can still be used as an approximation to determine whether or not flame temperature effects are having an impact on the interpretation of the results. In addition, recent works have shown that the C8 oxygenates studied have a similar flame temperature to that of diesel [12,13].

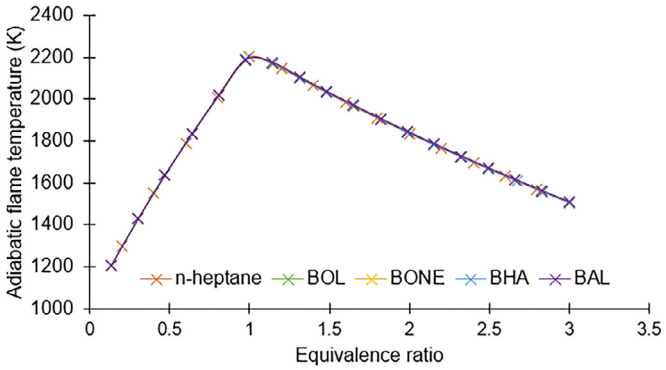

Fig. 7. Adiabatic flame temperature for the different fuels studied in this work, obtained from simulations made using the chemical equilibrium program Gaseq.

In order to determine the adiabatic flame temperature, thermochemical simulations were performed in this work for all the blends using the chemical equilibrium program Gaseq and considering ten species [27]. The initial conditions for the simulation were the ambient operating conditions obtained after chemical preheating of the chamber, as described in Section 2 (940 K ambient temperature, 25 bar ambient pressure, and 10% oxygen concentration). Heptane (normal) was used as a representative for diesel in the simulations, as it has been used in other studies as a large component of diesel surrogates [28]. NASA polynomials obtained from MIT's reaction mechanism generator were used as thermochemical inputs for the blends [29]. The simulation was run under adiabatic and constant volume conditions; the calculated results of the adiabatic flame temperature over a wide range of equivalence ratios for all the blends are presented in Fig. 7. The adiabatic flame temperature did not deviate significantly over a wider range of equivalence ratios for the different blends considered, hence the SINL derived from the experiments has been used as an indicator of soot concentration.

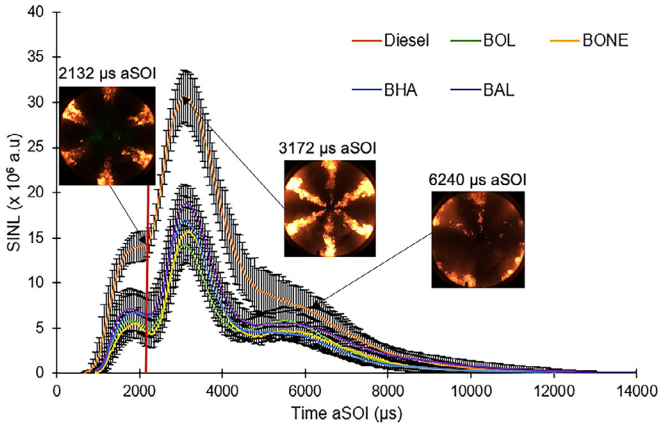

Fig. 8. Variation of the SINL with time for diesel and the blends studied. The error bars cover two standard deviations from the mean and the images presented are samples from a diesel injection event.

3.3. Sooting propensity

The spatially integrated natural luminosity (SINL) for diesel and all the blends is shown in Fig. 8. The SINL is the cumulative sum of the pixel's intensity (from the soot's natural luminosity) for different instants in time. The SINL in Fig. 8 is presented for all the six spray flames that were detected through the optical window. In addition to the temporal evolution of soot in Fig. 8, the spatial development of soot at different time instants is presented in Fig. 9 for diesel and for the blends studied.

Qualitatively, the global SINL trends were similar for all the fuels studied. Initially during the fuel injection period, the SINL increased until it reached the first peak, around the point in time when the fuel injection terminated. Thereafter, oxidation reactions started to become important, shown by the decrease in SINL. After a certain period, a minimum was reached for the oxygenates and a turning point for diesel. Then, the SINL started to increase again until it reached a second, larger peak. Thereafter, oxidation reactions dominated until the EOC. The SINL from the SOC to the first peak corresponds to reactions that are closely coupled to the spray dynamics and are mostly momentum-driven, whereas the SINL from the minimum (after the first peak) to the second peak corresponds to reactions occurring after the spray injection has ceased and the spray flame is no longer driven by the momentum of the fuel spray. These two scenarios are discussed separately in the two subsections below: Section 3.3.1 discusses the SINL from the SOC to the minimum after the first peak, and Section 3.3.2 discusses the SINL thereafter until the EOC. The red line in the graph in Fig. 8 and in the set of images in Fig. 9 delineates both time periods.

3.3.1. Sooting propensity in momentum-aided spray flames

During the fuel injection period, combustion dynamics are controlled by the spray momentum, and there is a constant feeding of fuel into the system. As combustion developed, the soot intensity increased until it reached its first local maxima, around 1800 µs aSOI, as seen in Fig. 8, and as seen in Fig. 9 ii) to iii). By taking the derivative from the SOC to the minimum (point of inflection) after the first local maxima, it is possible to explore the soot formation rates of diesel and the different fuel blends, as shown in Fig. 10. In order to smooth out the noise in the signal, a moving average of four data points was applied to the data sets. It can be seen from Fig. 10 that the rate of change of SINL is consistently larger for diesel, indicating a faster soot formation rate. For the oxygenates, even though the rate of SINL change was initially similar for all, eventually BAL reached a larger peak in the rate of change, followed by BHA, and by BONE and BOL. This is an interesting finding because even though the differences between the oxygenates are minor when compared to the differences between the oxygenates and diesel, it is not only the amount of soot that is affected by the different oxygenates but also the rate of soot formation.

For the oxygenates, the first SINL peak was reached at ~ 1800 µs aSOI (just before the actual end of injection at ~ 1900 µs), indicated by the point in time the derivative reached zero. For diesel this happened slightly later, at a time of ~ 2000 µs aSOI, showing that soot formation reactions were not only faster, but also more prolonged in time. Thereafter for diesel, the derivative remained near zero but did not become negative, indicating a negligible rate of change. This indicates that soot formation reactions were still dominant over oxidation ones but were less intense than when the fuel was been injected. For the oxygenates, the decrease in SINL rate continued until it became negative, indicating a change in slope of the SINL and also indicating that oxidation reactions become predominant. This can be seen in Fig. 8 where, after injection terminated, the SINL for the blends decreased between 1850 µs and 2100 µs aSOI, indicating that soot oxidation reactions increased over formation ones. This continued until at ~ 2200 µs aSOI a local minimum was encountered—point beyond which soot formation reactions overcame oxidation processes and the SINL rate became positive once more.

Fig. 8 shows that for the first SINL peak all blends reduced soot significantly relative to diesel. This reduction was approximately 62% for BONE, 60% for BOL, 53% for BHA, and 50% for BAL. The total area under the SINL curve in Fig. 8 from the SOC to the point where the first peak was encountered is shown in Fig. 11. The trend in soot reduction was similar to that for the first peak, albeit with reductions of 68% for BONE, 63% for BOL, 58% for BHA, and 56% for BAL. The differences in percentage reduction occur because the latter accounts for how much soot forms overall during a period of time. However, both of these data sets provide a useful reflection of how the oxygenates influence the development of soot during the spray injection. The observed soot suppression effects of the oxygenated blends can also be appreciated from the flame images shown from Fig. 9 i) to iv), where for the blends, high intensity sooting regions were confined to smaller spatial areas and were only observed in some sprays. On the other hand, for diesel, most sprays consistently showed higher intensity sooting regions that covered a wider spatial area in the spray flame. When looking at the flame evolution during this time, Fig. 9 iii) and iv) show that high intensity sooting areas were confined to regions closer to the chamber walls for the blends whereas for diesel high intensity sooting regions were distributed over a wider area of the spray. This contributed towards diesel's higher soot signal.

3.3.2. Sooting propensity in momentum-deficit spray flames

As the needle starts to ramp down, the fuel loses its momentum, and the liquid spray becomes wavy and undulated. The coupling between injection and flame becomes weak until it eventually decouples after the needle closes and the fuel fully vaporises. After the fuel had completely vaporised, just after ~ 2100 µs aSOI, soot started to form in the region between the nozzle and the sLOL, around the remains of the momentum-deficit spray. The SINL and the soot formation rate started to increase again for all fuels until the maximum peak was reached at around 3200 µs aSOI, as seen in Fig. 8. This increase in soot formation rate was caused by the combustion of near-nozzle fuel vapours and by the intensification of sooting reactions downstream of the sLOL. For this period there was no longer any fuel supply, and the spray combustion was no longer governed by the injection momentum.

The derivative of the second part of the SINL curve was obtained to help understand how soot formation and oxidation rates evolved for momentum-deficit sprays, and is shown in Fig. 12. The time period considered was between 2000 µs aSOI and 7000 µs

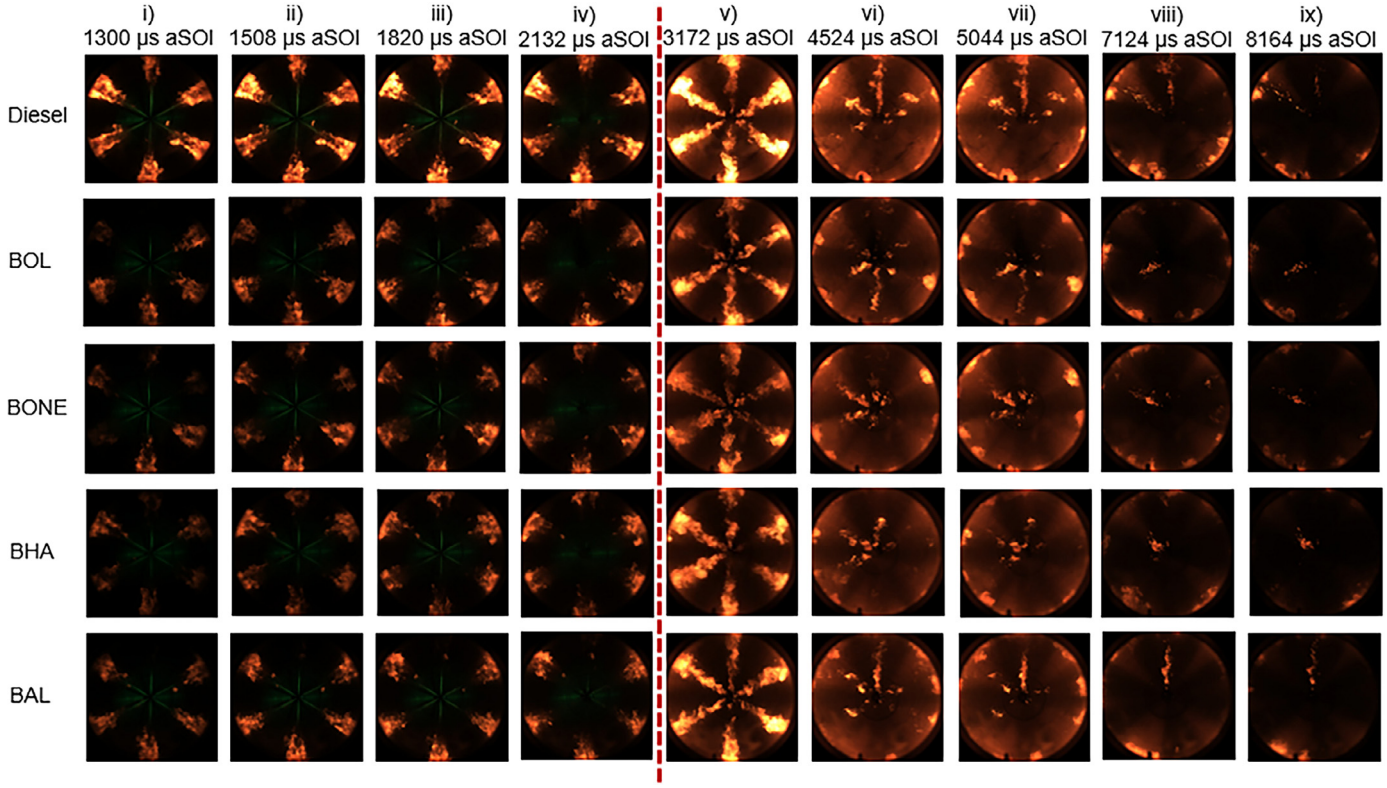

Fig. 9. High-speed images showing the development of soot throughout the combustion event for the different fuels studied. Lighter colours such as yellow and white indicate higher intensity (hot) soot regions, whereas darker ones indicate lower intensity (cool) soot regions.

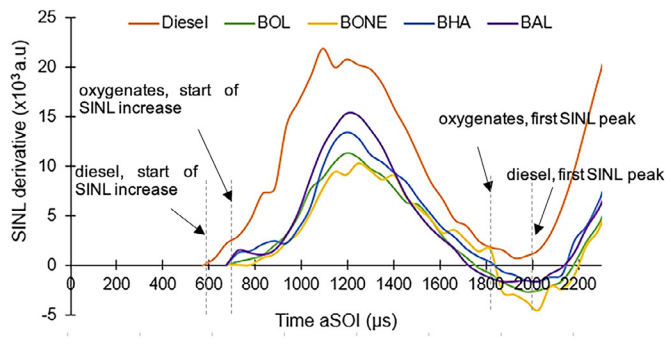

Fig. 10. SINL derivative with time from SOC to the minimum reached after the 1st SINL peak (~ 2300 µs).

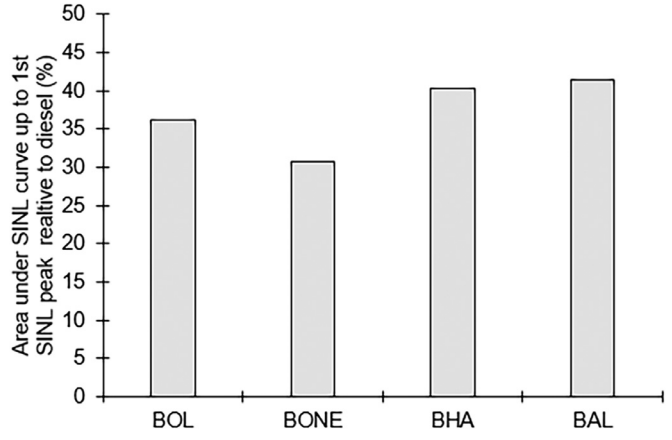

Fig. 11. Area integrated under SINL graph from the SOC to the 1st peak relative to diesel.

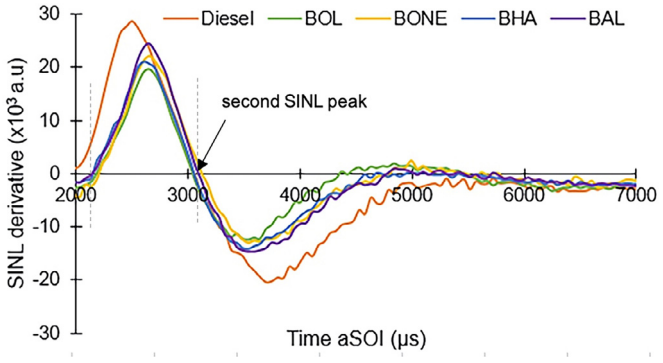

Fig. 12. SINL derivative with time from ~ 2300 µs to the end of main oxidation reactions.

aSOI. Before 3000 µs aSOI, diesel consistently showed the largest soot formation rate. All oxygenated blends had a similar rate to one another except at the peak of the derivative, where BAL showed the largest value followed by BONE, BHA, and BOL. At around 3200 µs aSOI, the derivatives for all fuels reached zero, and this corresponds to the point at which the maximum SINL was attained. Matching the injection profile and the LCV of the fuels caused soot to peak at the same point in time, and this peak SINL coincided with the point in time when soot covered most of the field of view, as seen in Fig. 9 v). At the maximum SINL peak, relative to diesel, the blends achieved a reduction of 49% for BONE, 54% for BOL, 45% for BHA, and 39% for BAL. When accounting for the area under the SINL curve between the 1st peak and the 2nd peak, the reductions relative to diesel were of 62% for BONE, 65% for BOL, 58% for BHA, and 49% for BAL, yielding a trend with increasing sooting propensity of BOL < BONE < BHA < BAL, as shown in Fig. 13. When comparing these results to the ones obtained in the previous section, one can see that during this

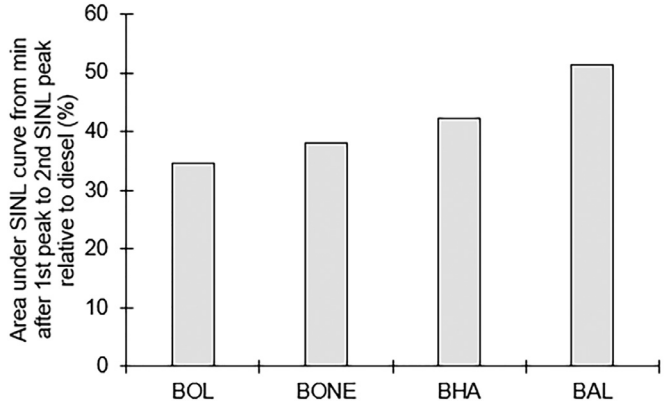

Fig. 13. Area integrated under SINL graph from the minimum after 1st peak to the 2nd peak relative to diesel.

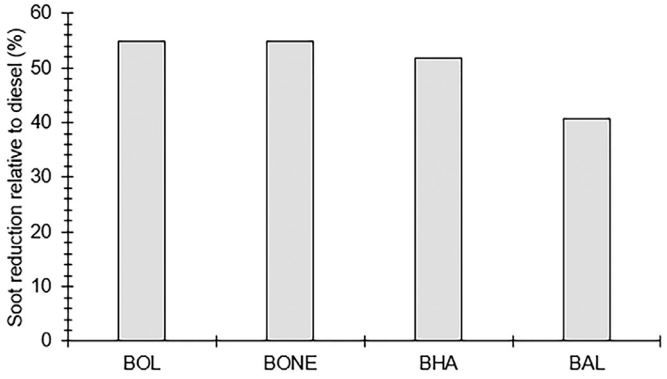

Fig. 14. Soot reduction of the oxygenated blends relative to diesel, obtained by integrating the SINL curve presented in Fig. 8.

spray momentum-deficit period, even though the oxygenates still reduced the sooting propensity relative to diesel significantly, their reduction was in general less than that attained during the spray momentum-aided period.

For diesel, the region between the wall and the nozzle was fully covered with high intensity soot for all the sprays, with 32% ± 4.5% of the total flame area covered with intensities holding at least 75% of the maximum flame intensity, Fig. 9 v). This was not the case for the blends, where some sprays even had regions that were not fully covered with soot, as pointed out by the arrows in Fig. 9 v). For the blends, the sooting regions had a relatively lower intensity, and those regions with a higher intensity remained confined to the spray head. On average, the flame area covered by high intensity regions of at least 75% of the maximum flame intensity was 12.0% ± 5.7% for BAL, 9.3% ± 5.2% for BHA, 8.1% ± 4.8% for BONE and 5.5% ± 1.9% for BOL. For diesel, all six sprays consistently showed higher sooting intensities, and these covered a wider area, indicating that intensely sooting reactions were more distributed across the spray flame. This finding shows that fuelling with oxygenates not only changes the amount of soot that forms, but also its spatial distribution: with the oxygenates, the high intensity sooting regions concentrated towards the downstream locations in the spray. The mechanisms behind this behaviour is explored and discussed in Section 3.4.

After reaching the maximum SINL peak, beyond 3200 µs aSOI, soot oxidation exceeded formation, and the SINL decreased for all fuels until most soot had fully oxidised. The oxidation time estimated by comparing the time between the peak SINL and the EOC revealed that diesel took ~ 11,000 µs to oxidise, which was on average longer than any of the other blends. From the oxygenated blends, the fastest one to oxidise was BHA, taking ~ 9400 µs; followed by BONE, taking ~ 9500 µs; then by BAL, taking ~ 10,000 µs; and finally by BOL, taking ~ 10,200 µs. On average, all oxygenated blends enhanced the oxidation of soot relative to diesel, with BHA promoting the fastest oxidation and BOL the slowest one.

Later in the combustion process, after the peak SINL, Fig. 9 vii) shows that the central regions of the spray oxidised faster compared to the spray tips for all fuels, with soot lingering near the nozzle as well as near the wall. Thereafter, the formation of soot steadily decreased until ~ 5000 µs aSOI, Fig. 9 vii). The high-speed images revealed that soot pockets that form are transported from the wall towards the central region due to convective motion caused by the head vortex (as marked by the arrows in Fig. 9 vii)). It is known that as the flames approach the wall, vortices can form as a result flame-to-flame and flame-to-wall interactions, creating mixing zones that transport soot back towards the central region of the chamber [30,31]. This phenomenon was observed for all fuels, showing that the evolution in spray dynamics is similar for different fuels. It is interesting to note from Fig. 9 vii) to viii), that small blobs of soot formed in the vicinity of the nozzle, when oxidation reactions were well underway for the main bulk of the flame. This is thought to be caused by the combustion and sooting of end of injection fuel expulsions, which have also been noted in [32]. This partly contributes to the slight increase in SINL signal observed in Fig. 8 between 5000 µs and 6000 µs aSOI. Eventually with time, oxidation reactions consumed the remaining pockets of soot until the EOC, as seen from Fig. 9 viii) to ix).

Overall, when integrating the SINL, the sooting tendency increased in the order of ketone ≈ alcohol < ester < aldehyde < diesel, with an average soot reduction relative to diesel of 55%, 55%, 52%, and 41%, respectively, as shown in Fig. 14. It is noted that these results refer to the generation of soot in the CVC as indicted by natural luminosity. In an engine, soot will also be burnt out during different stages of the cycle, so differences in engine-out soot between the fuels are likely to be less than the differences indicated by natural luminosity. In addition, the ubiquity of diesel particulate filters in current vehicles means that differences in tailpipe-out soot between the fuels may be smaller still. However, because slow soot burn-out can have a detrimental impact on engine efficiency [33], it remains desirable to minimise in-cylinder soot generation.

It is important to note that to obtain the same CN for all blends whilst keeping the oxygen content the same (Table 1), different percentages of isododecane and n-dodecane were used to form ternary blends of varying concentrations, with a maximum variation of 16% for the former, and a maximum variation of 17% for the latter. It is known that branched alkanes (such as isododecane) tend to produce more soot than their linear counterparts (such as n-dodecane), as they decompose to larger alkenes, which further decompose to produce smaller alkynes that eventually form soot precursors [34,35]. Even though the effect of isododecane on soot formation could not be precisely quantified, and even though based on the trends observed it did seem to be playing a role, it is not thought to be completely negating the effects of chemical moieties of the different blends in soot reduction. This was confirmed by looking at the variation of isododecane concentration in the blends relative to the increase in SINL: even though BHA had 4% more isododecane concentration than BONE and 8% more than BOL, the increase in total SINL for BHA was only of 3% relative to BONE and BOL. If the concentration of isododecane played a major role in soot formation, differences in SINL increase of BHA relative to BOL and BONE would have been larger, in proportion to isododecane concentration. Quantifying to what extent chemical moiety affects soot reduction in the presence of branched alkanes for the blends devised could be an interesting point to explore in future works involving chemical modelling.

When comparing the overall sooting trend between diesel and the blends, the results show that soot reduction stems from dilution and chemical effects of the oxygenates, and not only from pre-mixing effects. Chemical effects on soot reduction are those where the fuel-bound oxygen and the moiety directly influence the chemical pathways leading to soot formation. Pre-mixing effects are those where the mixing time before combustion is altered, where more mixing time normally implies less soot formation. In our work, soot reduction was not solely due to pre-mixing, as matching the cetane number for diesel and the blends would have resulted in all fuels producing a similar amount of soot. From the results presented, it seems that the presence of oxygen content in the blends and the convolved effect of dilution were larger than moiety-specific effects, as the difference in soot between diesel and the blends was larger than any of the differences between the blends. Nonetheless, potential chemical decomposition pathways that might be causing the slight differences observed between moieties warrant discussion.

3.4. Hypotheses on chemical decomposition pathways

The actual chemical reaction pathways that lead to soot inhibition are not known due to the lack of chemical kinetic investigations of some of the long carbon-chain oxygenated compounds considered. Detailed kinetic modelling works are required to explore the details of the chemical pathways responsible for soot inhibition of these long carbon-chain oxygenated fuel blends. The experimental data acquired from this work can be useful to help on the development of such chemical reaction mechanisms. In this work, preliminary hypotheses have been proposed based on the bond dissociation energy of the oxygenated compounds as well as on the outcome of previous works [13,36–42]. The aim is to gain an understanding of the small differences observed in sooting propensity between the oxygenated blends. The hypotheses proposed below help elucidate why different moieties soot to a different extent in the blends. These hypotheses are discussed focusing on moiety effects, but the influence of the branched component, isododecane, and the linear component, n-dodecane, in the blend should not be negated, as all the components present in the blend will have, to a greater or a lesser extent, an influence on soot formation and oxidation.

The aldehyde blend, BAL, showed the highest sooting tendency of all the oxygenated blends, but it still achieved a reduction of 41% in total SINL when compared to diesel. In terms of overall reduction relative to diesel, besides dilution and oxygen effects, the carbonyl group ($C = O$) present in the aldehyde blend is known to have a higher bond energy than the adjacent bonds [42]. Thus, the C atom attached to the O of the carbonyl group via a double bond is least likely to participate in soot forming reactions but instead escape as CO and CO_2. This effect has been observed in other works, where octanal was studied neat (albeit at much higher temperatures) [13]. The increase in SINL of BAL relative to the other oxygenates could be partly attributed to the higher amount of isododecane content in BAL compared to the other blends (Table 1), which might be favouring the formation of soot precursors and eventually leading to a slightly higher SINL. The higher SINL could also be influenced by the location of the carbonyl group towards the end of the carbon-chain, which does not effectively break down the remaining long alkyl chains that recombine into different precursors. Based on the oxidation time taken for BAL (~ 10,000 µs), it also seems that the soot produced by BAL had lesser oxidative reactivity, delaying the oxidation of soot and thereby contributing to the overall larger SINL values.

The next highest sooting blend was BHA, which achieved an overall reduction of 52% when compared to diesel. It showed a marginally higher sooting tendency than BONE and BOL, which could be a result of the inefficient use of the two oxygen atoms in the fuel structure (C - O and $C = O$) leading to the formation of CO_2 [37–39]. Out of all the blends, BHA showed the shortest oxidation time from peak SINL to EOC, indicating that BHA had a higher potential for soot oxidative reactivity. Previous works have shown that different fuels can produce soot with different nanostructures, leading to different oxidation rates, with more curved and more disordered soot structures leading to a higher reactivity [40]. Thus, it could also be that soot morphology differs for different oxygenates, hence different oxidation rates. Future works on soot morphology and detailed reaction mechanisms can provide additional insights on the soot oxidative characteristics of BHA and the other oxygenated blends.

On average, BOL and BONE had a similar SINL, with both blends achieving a total SINL reduction relative to diesel of 55%. This was despite BONE having 4% more isododecane concentration than BOL, which again shows that even though isododecane concentration might be playing a role on soot formation, its effect was not dominant. BONE's decomposition pathway could be similar to that for BAL, in terms of the carbonyl bond trapping the carbon. However, the more central location of the $C = O$ bond in octanone could be aiding in a more efficient break-down of the long carbon-chain molecule to smaller compounds to reduce soot formation. For alcohols such as octanol, reduction in soot has been previously attributed to dilution rather than moiety-specific effects [41], as the -OH group tends to be removed to form H_2O and thus may not effectively participate in any soot-trapping reactions. Overall, BOL and BONE seemed to have the largest effect on total soot reduction out of the four C8 blends studied.

4. Conclusions

Fuel investigations of high-pressure sprays were performed to study the influence of different C8 oxygenate moieties on soot reduction when blended with n-dodecane and isododecane. The ternary blends were designed to have the same oxygen content by mass of 2.5% and a matching cetane number of 52. The fuels were injected at high pressures using a multi-hole injector into a constant volume chamber maintained at a high pressure and temperature, and the soot natural luminosity was measured at high speeds. The adiabatic flame temperatures were obtained for the ternary blends by using a chemical reaction program, and their similarity confirmed that the outcome of the SINL study could be related to soot concentration.

In terms of the combustion characteristics based on the study of soot, all oxygenates delayed the first appearance of soot, which indicates that soot-forming conditions were being suppressed from the early combustion stages by the oxygenates. The differences amongst the oxygenates were smaller than those between the oxygenates and diesel, showing that from the early combustion stages both dilution and oxygen content effects are dominant over moiety-specific effects. Nevertheless, the effect of different moieties on overall soot processes cannot be negated. The soot from the blends oxidised ~ 10% faster than diesel. Relative to diesel, all blends had an approximately 40% longer sLOL, indicating that oxygen concentration in the blend suppressed the accumulation of soot and its precursors to a more downstream location, delaying the onset of stable sooting reactions. This reduces the spatial and temporal lengths that soot has to grow, making it easier to oxidise.

The analysis of SINL signals revealed that initially the soot intensity increased as the fuel was injected, and thereafter decreased for the blends as oxidation reactions took over. For diesel, the increase in soot intensity continued after the end of injection albeit at a slower rate. During this first part of the SINL curve, the decrease in SINL relative to diesel was of 68% for BONE, 63% for BOL, 58% for BHA, and 56% for BAL. As the remaining fuel vapor-

ised and started to combust, soot reactions intensified and reached their peak at around 3200 µs aSOI. After reaching the peak, oxidation reactions took over and the SINL decreased until the EOC. When integrating the whole SINL signal, the sooting tendency of the fuels increased in the order of ketone ≈ alcohol < ester < aldehyde < diesel, with an average soot reduction relative to diesel of 55%, 55%, 52%, and 41%. Under high pressure diesel-like spray flame conditions, soot reduction of the blends was, to a large extent, caused by the combined effect of oxygen content in the fuel and dilution effects, as the differences were consistently larger between diesel and the oxygenates than between the oxygenates themselves. Nonetheless, the small differences between the oxygenates indicates that the moiety does have an effect, but it is small for high-pressure practical applications under the conditions studied.

Declaration of Competing Interest

The authors declare that they have no known competing financial interests or personal relationships that could have appeared to influence the work reported in this paper.

Acknowledgements

This work was supported financially by the Engineering and Physical Science Research Council (EPSRC) and is gratefully acknowledged.

References

[1] R.D. Reitz, H. Ogawa, R. Payri, T. Fansler, S. Kokjohn, Y. Moriyoshi, A.K. Agarwal, D. Arcoumanis, D. Assanis, C. Bae, K. Boulouchos, M. Canakci, S. Curran, I. Denbratt, M. Gavaises, M. Guenthner, C. Hasse, Z. Huang, T. Ishiyama, B. Johansson, T.V. Johnson, G. Kalghatgi, M. Koike, S.C. Kong, A. Leipertz, P. Miles, R. Novella, A. Onorati, M. Richter, S. Shuai, D. Siebers, W. Su, M. Trujillo, N. Uchida, B.M. Vaglieco, R.M. Wagner, H. Zhao, IJER editorial: the future of the internal combustion engine, Int. J. Engine Res. 21 (2020) 3–10.
[2] J. Benajes, J. Martín, A. García, D. Villalta, A. Warey, In-cylinder soot radiation heat transfer in direct-injection diesel engines, Energy Convers. Manage. 106 (2015) 414–427.
[3] T.C. Bond, S.J. Doherty, D.W. Fahey, P.M. Forster, T. Berntsen, B.J. DeAngelo, M.G. Flanner, S. Ghan, B. Kärcher, D. Koch, S. Kinne, Y. Kondo, P.K. Quinn, M.C. Sarofim, M.G. Schultz, M. Schulz, C. Venkataraman, H. Zhang, S. Zhang, N. Bellouin, S.K. Guttikunda, P.K. Hopke, M.Z. Jacobson, J.W. Kaiser, Z. Klimont, U. Lohmann, J.P. Schwarz, D. Shindell, T. Storelvmo, S.G. Warren, C.S. Zender, Bounding the role of black carbon in the climate system: a scientific assessment, J. Geophys. Res. Atmos. 118 (2013) 5380–5552.
[4] D.D. Das, P.C. St. John, C.S. McEnally, S. Kim, L.D. Pfefferle, Measuring and predicting sooting tendencies of oxygenates, alkanes, alkenes, cycloalkanes, and aromatics on a unified scale, Combust. Flame 190 (2018) 349–364.
[5] W. Park, S. Park, R.D. Reitz, E. Kurtz, The effect of oxygenated fuel properties on diesel spray combustion and soot formation, Combust. Flame 180 (2017) 276–283.
[6] B. Kerschgens, L. Cai, H. Pitsch, B. Heuser, S. Pischinger, Di-n-buthylether, n-octanol, and n-octane as fuel candidates for diesel engine combustion, Combust. Flame 163 (2016) 66–78.
[7] G.D. Guerrero Peña, Y.A. Hammid, A. Raj, S. Stephen, T. Anjana, V. Balasubramanian, On the characteristics and reactivity of soot particles from ethanol–gasoline and 2,5-dimethylfuran-gasoline blends, Fuel 222 (2018) 42–55.
[8] J. Hwang, C. Bae, C. Patel, R.A. Agarwal, T. Gupta, A.Kumar Agarwal, Investigations on air-fuel mixing and flame characteristics of biodiesel fuels for diesel engine application, Appl. Energy 206 (2017) 1203–1213.
[9] M. Pelucchi, C. Cavallotti, E. Ranzi, A. Frassoldati, T. Faravelli, Relative reactivity of oxygenated fuels: alcohols, aldehydes, ketones, and methyl esters, Energy Fuels 30 (2016) 8665–8679.
[10] A. Jamrozik, W. Tutak, R. Gnatowska, Ł. Nowak, Comparative analysis of the combustion stability of diesel-methanol and diesel-ethanol in a dual fuel engine, Energies 12 (2019) 1–17.
[11] Z. Hong, D.F. Davidson, S.S. Vasu, R.K. Hanson, The effect of oxygenates on soot formation in rich heptane mixtures: a shock tube study, Fuel 88 (2009) 1901–1906.
[12] I. Ruiz-Rodriguez, R. Cracknell, M. Parkes, T. Megaritis, L. Ganippa, Experimental study of the effect of C8 oxygenates on sooting processes in high pressure spray flames, Combust. Flame 220 (2020) 235–246.
[13] I. Ruiz-Rodriguez, R. Cracknell, M. Parkes, T. Megaritis, L. Ganippa, Experimental study on the combustion characteristics of high-pressure octanal spray flames, Fuel 262 (2020) 1–9.
[14] R. Lemaire, D. Lapalme, P. Seers, Analysis of the sooting propensity of C-4 and C-5 oxygenates: comparison of sooting indexes issued from laser-based experiments and group additivity approaches, Combust. Flame 162 (2015) 3140–3155.
[15] A.J. Donkerbroek, M.D. Boot, C.C. Luijten, N.J. Dam, J.J. Meulen, Flame lift-off length and soot production of oxygenated fuels in relation with ignition delay in a DI heavy-duty diesel engine, Combust. Flame 158 (2011) 525–538.
[16] J. Preuß, K. Munch, I. Denbratt, Performance and emissions of long-chain alcohols as drop-in fuels for heavy duty compression ignition engines, Fuel 216 (2018) 890–897.
[17] Y. Ren, Z. Huang, H. Miao, Y. Di, D. Jiang, K. Zeng, B. Liu, X. Wang, Combustion and emissions of a DI diesel engine fuelled with diesel-oxygenate blends, Fuel 87 (2008) 2691–2697.
[18] E.J. Barrientos, M. Lapuerta, A.L. Boehman, Group additivity in soot formation for the example of C-5 oxygenated hydrocarbon fuels, Combust. Flame 160 (2013) 1484–1498.
[19] B. Heuser, T. Laible, M. Jakob, F. Kremer, S. Pischinger, C8-oxygenates for clean diesel combustion, SAE Tech. Paper 2014-01-1253 (2014) 1–20.
[20] M. Zubel, S. Pischinger, B. Heuser, Assessment of the full thermodynamic potential of C8-oxygenates for clean diesel combustion, SAE Int. J. Fuels Lubr. 10 (2017) 913–923.
[21] P. Majidian, M. Tabatabaei, M. Zeinolabedini, M.P. Naghshbandi, Y. Chisti, Metabolic engineering of microorganisms for biofuel production, Renew. Sustain. Energy Rev. 82 (2018) 3863–3885.
[22] J. Julis, W. Leitner, Synthesis of 1-octanol and 1,1-dioctyl ether from biomass-derived platform chemicals, Angewandte Chemie - Int. Edition 51 (2012) 8615–8619.
[23] M.K. Akhtar, H. Dandapani, K. Thiel, P.R. Jones, Microbial production of 1-octanol: a naturally excreted biofuel with diesel-like properties, Metab. Eng. Commun. 2 (2015) 69–76.
[24] BEIS, Digest of UK Energy Statistics (DUKES), London, 2018.
[25] C.J. Mueller, G.C. Martin, Effects of oxygenated compounds on combustion and soot evolution in a DI diesel engine: broadband natural luminosity imaging, SAE Int. J. Fuels Lubr. 111 (2002) 518–537.
[26] R. Hessel, Z. Yue, R. Reitz, M. Musculus, J. O'Connor, Guidelines for interpreting soot luminosity imaging, SAE Int. J. Engines 10 (2017) 1174–1192.
[27] C. Morley, Gaseq, (n.d.). http://www.gaseq.co.uk.
[28] W.J. Pitz, C.J. Mueller, Recent progress in the development of diesel surrogate fuels, Prog. Energy Combust. Sci. 37 (2011) 330–350.
[29] MIT, Reaction Mechanism Generator, (2018). rmg.mit.edu.
[30] J.E. Dec, D.R. Tree, Diffusion-flame/wall interactions in a heavy-duty DI diesel engine, SAE Int. J. Engines 110 (2001) 1599–1617.
[31] J. Eismark, M. Christensen, M. Andersson, A. Karlsson, I. Denbratt, Role of fuel properties and piston shape in influencing soot oxidation in heavy-duty low swirl diesel engine combustion, Fuel 254 (2019) 1–13.
[32] R. Pos, M. Avulapati, R. Wardle, R. Cracknell, T. Megaritis, L. Ganippa, Combustion of ligaments and droplets expelled after the end of injection in a multi–hole diesel injector, Fuel 197 (2017) 459–466.
[33] P.C. Bakker, R. Willems, N. Dam, B. Somers, C. Wakefield, M. Brewer, R. Cracknell, Investigation of late stage conventional diesel combustion - effect of additives, SAE Technical Paper 2018-01-1787. (2018) 1–6.
[34] C.S. McEnally, D.M. Ciuparu, L.D. Pfefferle, Experimental study of fuel decomposition and hydrocarbon growth processes for practical fuel components: heptanes, Combust. Flame 134 (2003) 339–353.
[35] A. Gomez, G. Sidebotham, I. Glassman, Sooting behavior in temperature-controlled laminar diffusion flames, Combust. Flame 58 (1984) 45–57.
[36] H. Ogawa, N. Miyamoto, M. Yagi, Chemical-kinetic analysis on PAH formation mechanisms of oxygenated fuels, SAE Technical Paper 2003-01-3190. (2003) 1–11.
[37] P. Pepiot-Desjardins, H. Pitsch, R. Malhotra, S.R. Kirby, A.L. Boehman, Structural group analysis for soot reduction tendency of oxygenated fuels, Combust. Flame 154 (2008) 191–205.
[38] J. Abboud, J. Schobing, G. Legros, A. Matynia, J. Bonnety, V. Tschamber, A. Brillard, G. Leyssens, P.Da Costa, Impacts of ester's carbon chain length and concentration on sooting propensities and soot oxidative reactivity: application to diesel and biodiesel surrogates, Fuel 222 (2018) 586–598.
[39] C.K. Westbrook, W.J. Pitz, P.R. Westmoreland, F.L. Dryer, M. Chaos, P. Osswald, K. Kohse-Höinghaus, T.A. Cool, J. Wang, B. Yang, N. Hansen, T. Kasper, A detailed chemical kinetic reaction mechanism for oxidation of four small alkyl esters in laminar premixed flames, Proc. Combust. Inst. 32 (2009) 221–228.
[40] H. Ghiassi, P. Toth, J.S. Lighty, Sooting behaviors of n-butanol and n-dodecane blends, Combust. Flame 161 (2014) 671–679.
[41] C.S. McEnally, L.D. Pfefferle, Sooting tendencies of oxygenated hydrocarbons in laboratory-scale flames, Environ. Sci. Technol. 45 (2011) 2498–2503.
[42] G.Da Silva, J.W. Bozzelli, Enthalpies of formation, bond dissociation energies, and molecular structures of the n-aldehydes (acetaldehyde, propanal, butanal, pentanal, hexanal, and heptanal) and their radicals, J. Phys. Chem. A 110 (2006) 13058–13067.